Polysaccharides induce deep-sea *Lentisphaerae* strains to release chronic bacteriophages

Chong Wang[1,2,4], Rikuan Zheng[1,2,4], Tianhang Zhang[1,2,3,4], Chaomin Sun[1,2,3,4*]

[1]CAS and Shandong Province Key Laboratory of Experimental Marine Biology & Center of Deep Sea Research, Institute of Oceanology, Chinese Academy of Sciences, Qingdao, China.

[2]Laboratory for Marine Biology and Biotechnology, Qingdao Marine Science and Technology Center, Qingdao, China.

[3]College of Earth Science, University of Chinese Academy of Sciences, Beijing, China.

[4]Center of Ocean Mega-Science, Chinese Academy of Sciences, Qingdao, China.

[*] Corresponding author

Chaomin Sun

Tel.: +86 532 82898857; fax: +86 532 82898857.

E-mail address: sunchaomin@qdio.ac.cn

Key words: deep-sea virus, polysaccharides, bacteriophages, auxiliary metabolic genes, carbon cycle

Running title: Induction of chronic bacteriophages by polysaccharides

Abstract

Viruses are ubiquitous in nature and play key roles in various ecosystems. Notably, some viruses (e.g. bacteriophage) exhibit alternative life cycles, such as chronic infections without cell lysis. However, the impact of chronic infections and their interactions with the host organisms remains largely unknown. Here, we found for the first time that polysaccharides induced the production of multiple temperate phages infecting two deep-sea *Lentisphaerae* strains (WC36 and zth2). Through physiological assays, genomic analysis, and transcriptomics assays, we found these bacteriophages were released via a chronic style without host cell lysis, which might reprogram host polysaccharide metabolism through the potential auxiliary metabolic genes (AMGs). The findings presented here, together with recent discoveries made on the reprogramming of host energy-generating metabolisms by chronic bacteriophages, shed light on the poorly explored marine virus-host interaction and bring us closer to understanding the potential role of chronic viruses in marine ecosystems.

Introduction

Viruses are the most abundant and genetically diverse biological entities on this planet (Suttle, 2007), and potentially play a role in shaping microbial abundances, community structure, and the evolutionary trajectory of core metabolisms (Sullivan et al., 2006; Samson et al., 2013; Zimmerman et al., 2020). The effect of bacteriophages (viruses that infect bacteria) on their specific hosts and within the microbial community is largely determined by their lifestyle. Traditionally, most bacteriophage life cycles are classified as being either lytic or lysogenic (Du Toit, 2017). During the lytic cycle, phages hijack the host's metabolic machinery for replication of their own genome and the production of progeny particles that are released through lysis. By contrast, during lysogeny, phages integrate their genomes into the host chromosome (or exist in the extrachromosomal form) and enter a dormant state, with the potential to re-enter a lytic cycle and release progeny by environmental changes at a later stage. Currently, more and more attention has been paid to chronic life cycles where bacterial growth continues despite phage reproduction (Hoffmann Berling and Maze, 1964), which was different from the lysogenic life cycle that could possibly lyse the host under some specific conditions. During a chronic cycle, progeny phage particles are released from host cells via extrusion or budding without killing the host (Putzrath and Maniloff, 1977; Russel, 1991; Marvin et al., 2014), instead of lysis of the host cell. Chronic infections are common among eukaryotic viruses (Godkin and Smith, 2017), however, to our best knowledge, only few phages have been described for prokaryotes in the pure isolates up to date (Roux et al., 2019; Alarcón-Schumacher et al., 2022; Liu et al., 2022). The best-studied examples of chronic infection are those from filamentous ssDNA (single-stranded DNA) phages that to date have primarily been identified in the order *Tubulavirales*, which currently involves three families (*Inoviridae*, *Paulinoviridae* and *Plectroviridae*) (Ackermann, 2007, 2009; Knezevic et al., 2021; Chevallereau et al., 2022). One of the most distinctive features of inoviruses is their ability to establish a chronic infection whereby their genomes may either integrate into the host chromosome or reside within the cell in a non-active form, and

inoviruses particles are continuously released without killing the host. In addition, tailless phages enclosed in lipid membrane are also released from hosts during chronic life cycles (Liu et al., 2022). Recent studies indicate that chronic cycles are more widespread in nature than previously thought (Mäntynen et al., 2021), and the abundance of inoviruses in ecosystem may have been far underestimated (Roux et al., 2019). Therefore, a large percentage of phages in nature are proposed to replicate through chronic life cycles, but whether chronic cycles are associated with specific environments or ecological conditions remains to be thoroughly explored (Chevallereau et al., 2022).

Marine ecosystems always influence the operating conditions for life on earth via microbial interaction networks (Falkowski et al., 1998; Faust and Raes, 2012; Wigington et al., 2016), which are modulated by viruses through impacting their lifespan, gene flow and metabolic outputs (Suttle, 2005). A majority of these viruses are bacteriophages, which exist widely in oceans and affect the life activities of microbes (Breitbart, 2012; Roux et al., 2016; Gregory et al., 2019; Dominguez-Huerta et al., 2022). In addition to core viral genes encoding viral structural proteins (Brum et al., 2016), bacteriophages also encode various auxiliary metabolic genes (AMGs) (Brum and Sullivan, 2015) that provide supplemental support to key steps of host metabolism. For instance, AMGs of marine bacteriophages have been predicted to be involved in photosynthesis (Mann et al., 2003), nitrogen cycling (Ahlgren et al., 2019; Gazitúa et al., 2021), sulfur cycling (Anantharaman et al., 2014; Roux et al., 2016), phosphorus cycling (Zeng and Chisholm, 2012), nucleotide metabolism (Sullivan et al., 2005; Dwivedi et al., 2013; Enav et al., 2014), and almost all central carbon metabolisms in host cells (Hurwitz et al., 2013). However, AMGs of chronic phages have not been reported. Thus, it is worth exploring whether chronic phages could carry AMGs and assist host metabolism during chronic infection.

The deep sea harbors abundant and undiscovered viruses, which potentially control the metabolism of microbial hosts and influence biogeochemical cycling (Li et al., 2021). However, due to the vast majority of deep-sea microbes cannot be cultivated in the laboratory, most bacteriophages could not be isolated. Thus, it is of

great significance to further identify unknown phages in the deep sea and explore their relationship with microbial hosts and even marine ecosystems. Here, we report that polysaccharides can induce deep-sea *Lentisphaerae* bacteria (difficult-to-cultivate microorganisms) to release some chronic bacteriophages. These chronic bacteriophages might assist host polysaccharides metabolism via corresponding potential AMGs.

Results and Discussion

Polysaccharides promote the growth of deep-sea *Lentisphaerae* strain WC36 and stimulate the expression of phage-associated genes

As a primary carbon source, polysaccharides are a ubiquitous energy source for microorganisms in both terrestrial and marine ecosystems (Zheng et al., 2021a). In our previous work, we successfully isolated a novel *Bacteroidetes* species through a polysaccharide degradation-driven strategy from the deep-sea cold seep (Zheng et al., 2021a). Of note, using the same approach and deep-sea sample replicates, we also cultured a bacterial strain WC36 that was identified as a member of the phylum *Lentisphaerae* by 16S rRNA gene sequence-based phylogenetic analysis (Figure 1A). As expected, growth assays showed that two kinds of polysaccharides including laminarin and starch could promote strain WC36 growth (Figure 1B). In particular, supplementation of 10 g/L laminarin and 10 g/L starch in rich medium resulted in ~7-fold and ~4-fold growth promotion respectively compared to cultivation in rich medium (Figure 1B).

To explore the reasons behind this significant growth promotion by polysaccharide supplementation, we performed a transcriptomic analysis of strain WC36 cultured in rich medium supplemented either with or without 10 g/L laminarin for 5 days and 10 days. In addition to the up-regulation of genes related to glycan transport and degradation, when 10 g/L laminarin was added in the rich medium, the most upregulated genes were phage-associated (e. g. phage integrase, phage portal protein) (Figure 1C and Table 1), which were expressed at the background level in the rich medium alone. Consistently, RT-qPCR results (Figure 1D) confirmed

upregulation of some genes encoding phage-associated proteins, as shown in Figure 1C. Therefore, we speculate that the metabolism of polysaccharides in strain WC36 might be closely connected with the phage production.

Table 1. Annotations and fold-changes of the transcriptome data of *Lentisphaerae* strain WC36 cultured in rich medium supplemented with or without 10 g/L laminarin. "Rich" indicates strain WC36 cultivated in rich medium; "Lam" indicates strain WC36 cultivated in rich medium supplemented with 10 g/L laminarin.

Gene_id	Lam	Rich	Log_2 fold change	*P*-value	Gene annotation
LJT99_00010	34.66133	1.947696	4.047436	0.000885	Phage tail protein
LJT99_00015	59.24968	5.003597	3.5227	4.30E-05	Phage portal protein
LJT99_00030	191.9747	7.854776	4.585701	1.74E-14	Phage tail tape measure protein
LJT99_00055	69.08332	0.3268	7.239027	5.06E-07	Phage virion morphogenesis protein
LJT99_00075	39.57964	5.818312	2.726103	0.003149	Phage major capsid protein
LJT99_00080	64.1666	1.13323	5.654168	7.40E-07	Phage capsid protein
LJT99_02570	14.98313	1.39E-17	8.242446	0.040965	Phage integrase
LJT99_05290	59.24968	0.727225	6.096258	2.40E-06	Phage terminase large subunit
LJT99_05300	39.57964	0.727225	5.511892	0.00012	Phage minor capsid protein
LJT99_05340	49.41521	3.170158	3.896062	2.30E-05	Phage portal protein
LJT99_07085	49.41521	2.558919	4.19071	3.37E-05	Phage portal protein
LJT99_07095	59.24968	1.947696	4.824191	7.40E-07	Phage terminase large subunit
LJT99_07125	59.24968	3.577629	3.991305	3.68E-06	Phage integrase
LJT99_09950	64.1666	5.410965	3.528071	1.70E-05	Phage tail tape measure protein
LJT99_10035	78.91632	9.483688	3.033143	2.89E-05	Phage terminase large subunit
LJT99_14585	69.08332	26.58123	1.366501	0.040756	Phage head-tail adapter protein
LJT99_15275	44.49759	0.727225	5.681619	4.78E-05	Phage integrase
LJT99_15295	88.74881	3.781357	4.498866	9.38E-09	Phage terminase large subunit
LJT99_15305	49.41521	3.577629	3.728509	0.000117	Phage portal protein
LJT99_15310	78.91632	15.18374	2.361653	0.00034	Phage major capsid protein
LJT99_15370	24.82336	4.188794	2.510263	0.030348	Phage major tail tube protein
LJT99_01210	305.0198	11.31601	4.735088	1.56E-17	Type VI secretion system protein VipA
LJT99_01215	737.5197	9.687289	6.230941	1.36E-28	Type VI secretion system protein EvpB
LJT99_01245	39.57964	1.947696	4.239825	4.78E-05	Type VI secretion system baseplate subunit TssK
LJT99_01250	177.2291	6.632948	4.709658	2.15E-14	Type VI secretion system protein IcmF
LJT99_02010	93.66489	28.61632	1.700863	0.00488	Bacterial type II and III secretion system protein
LJT99_02015	64.1666	23.1215	1.459804	0.029185	Type II secretion system (T2SS), protein E
LJT99_02020	103.4968	16.40502	2.643067	2.06E-05	Type II secretion system (T2SS), protein F
LJT99_12295	15122.75	3729.384	2.01964	2.19E-06	Type II secretion system GspH family protein
LJT99_15330	54.33257	1.743985	4.847018	2.40E-06	Type VI secretion system protein

Polysaccharides induce the production of bacteriophages in *Lentisphaerae* strain WC36

To test our hypothesis that polysaccharides might induce strain WC36 to release bacteriophages, we grew strain WC36 in rich medium supplemented with or without laminarin or starch and isolated bacteriophages from the cell suspension supernatant according to established standard protocols (Lin et al., 2012). Based on the growth curve of strain WC36, we found that the growth rate of strictly anaerobic strain WC36 was relatively slow. Therefore, different to the typical sampling time (24 h) for bacteriophage isolation from other bacteria (Jiang and Paul, 1996; Weinbauer et al., 1999), we selected a longer sampling time (10 days) to extract bacteriophages. TEM observation showed that many different shapes of phage-like structures indeed existed in the supernatant of WC36 cells cultured in rich medium supplemented with laminarin (Figure 2A, panels II-IV) or starch (Figure 2A, panels V-VIII). In contrast, we did not observe any phage-like structures in the supernatant of WC36 cells cultured in rich medium (Figure 2A, panel I). We also tested and confirmed that there were not any phage-like structures in rich medium supplemented with 10 g/L laminarin alone (Figure 2—figure supplement 1A) or in 10 g/L starch alone (Figure 2—figure supplement 1B), ruling out the possibility of phage contamination from the polysaccharides (laminarin/ starch). These results suggest that polysaccharides indeed stimulate the production of various bacteriophages from strain WC36. Correspondingly, in the presence of laminarin, different forms of bacteriophages were observed by TEM, with filamentous ones dominant (Figure 2A). The length of these filamentous phages was about ~0.4 μm to ~8.0 μm (Figure 2A, panel II), and the size of the hexagonal phages was less than 100 nm (Figure 2A, panel IV). In the presence of starch, in addition to filamentous and hexagonal phages (Figure 2A, panels V, VI, and VIII), we also observed a kind of icosahedral *Microviridae*-like phage with a diameter of 25-30 nm (Figure 2A, panel VII).

Given that we found bacteriophages in cultures of strain WC36, we next sought to explore whether bacteriophages adhering to bacterial cells could be observed. To this end, we checked the morphology of strain WC36 in the absence or presence of

polysaccharides. As expected, with TEM we observed many filamentous phage-like structures around strain WC36 cells cultivated in rich medium supplemented with laminarin (Figure 2B, panel II) and starch (Figure 2B, panels III-IV). In contrast, we could not find any phage-like structures around strain WC36 cells cultivated in rich medium (Figure 2B, panel I). Meanwhile, we also checked the polysaccharides (laminarin/ starch) in rich medium directly by TEM and did not find any phage-like structures (Figure 2—figure supplement 2). Moreover, based on TEM observation of ultrathin sections of strain WC36 cultured in medium supplemented with polysaccharide, we even observed filamentous phages that were being released from or entering into host cells via a kind of extrusion or budding structure around bacterial cells (Figure 2C, panels II-IV; (Figure 2—figure supplement 3B, panels II-III), which were typical cellular structures in host cells used for chronic bacteriophage release (Marvin et al., 2014; Krupovic and Consortium, 2018). In contrast, phage-like structures with extrusions or buddings were not found in cells of strain WC36 cultivated in rich medium (Figure 2C, panel I; Figure 2—figure supplement 3B, panel I). Hence, these results collectively suggest that filamentous bacteriophages induced from deep-sea strain WC36 replicate in a chronic manner as reported previously (Chevallereau et al., 2022; Liu et al., 2022). However, the entry and exit of the hexagonal phages into the WC36 cells were not observed.

To further verify the release style of bacteriophages from strain WC36 in the presence of polysaccharide, we prolonged the incubation time of this strain up to 30 days in medium supplemented with 5 g/L or 10 g/L laminarin. Strain WC36 showed stable growth after it entered the stationary phase (Figure 3A). Regardless of whether the laminarin was present, the bacterial cells kept their cell shape intact, indicating they were still healthy after 30 days (Figure 2—figure supplement 3A, panels I-III). Apparently, the replication and release of bacteriophages in strain WC36 did not kill the host cell, consistent with the key feature of chronic bacteriophages (Howard-Varona et al., 2017). With an increase of culture time (5, 10, or 30 days) and laminarin concentration (5 or 10 g/L), the number of released bacteriophages increased (Figure 2—figure supplement 3A, panels IV-VI; Figure 3—figure

supplement 1, panels IV-IX). Specifically, the average number per microliter of filamentous phages (9.7, 29 or 65.3) extracted from the supernatant of strain WC36 cultured in rich medium supplemented with 10 g/L laminarin for 5, 10 or 30 days was higher than that cultured in rich medium supplemented with 5 g/L laminarin (4.3, 13.7 or 35.3) (Figure 3B). The average number per microliter of hexagonal phages (9, 30, 46.7) extracted from the supernatant of strain WC36 cultured in rich medium supplemented with 10 g/L laminarin for 5, 10 or 30 days was higher than that cultured in rich medium supplemented with 5 g/L laminarin (4, 11.3 or 17.7) (Figure 3C).

Polysaccharides promote the growth of deep-sea *Lentisphaerae* strain zth2 and induce bacteriophage production

To explore whether the production of bacteriophages induced by polysaccharide is an individual case, we further checked the effect of polysaccharides on another cultured deep-sea *Lentisphaerae* strain zth2. Strain zth2 was isolated by the same polysaccharide degradation-driven strategy as that used for strain WC36 (Zhang et al., 2022). 16S rRNA gene sequence similarity calculation using the NCBI server indicated that the closest relative of strain zth2 was strain WC36 (90.4%), which was lower than the threshold sequence identity (94.5%) for distinct genera (Yarza et al., 2014). Based on a maximum likelihood tree and similarity of 16S rRNA gene sequences, we propose that strain zth2 and WC36 are the type strains of two different novel genera, both belonging to the *Lentisphaeraceae* family, *Lentisphaerales* order, *Lentisphaeria* class. Consistently, laminarin indeed promoted the growth of strain zth2 (Figure 4A). Analysis of the differential transcriptome and RT-qPCR of strain zth2 cultured in either unsupplemented medium or with laminarin showed that many genes encoding critical factors associated with the phage life cycle were up-regulated (ranging from 4 to 200 fold) (Figure 4B, C and Supplementary file 1), suggesting that phages might also be involved in the utilization of laminarin by strain zth2, the same as in strain WC36.

To further confirm the existence of bacteriophages in the supernatant of strain zth2 cell suspension cultured in medium supplemented with polysaccharide, we

performed bacteriophage isolation from the supernatant of strain zth2 cultures followed by TEM. Indeed, many filamentous-, hexagonal- and icosahedral phages were clearly observed in the culture of strain zth2 grown in the presence of laminarin (Figure 4D, panels I-III) and starch (Figure 4D, panels IV-V), but not in rich medium short of polysaccharide (Figure 4D, panel VI). This suggests that bacteriophages were induced by supplementation of polysaccharide to strain zth2.

In addition, transcriptome and RT-qPCR results showed that genes encoding bacterial secretion system-related proteins were up-regulated in strains WC36 (Figure 4—figure supplement 1A, B) and zth2 (Figure 4—figure supplement 1C, D) cultured in medium supplemented with laminarin. It has been reported that filamentous phages utilize host cell secretion systems for their own egress from bacterial cells (Davis et al., 2000; Bille et al., 2005). Therefore, the filamentous phages induced from strains WC36 and zth2 might also get in and out of host cells using bacterial secretion systems. Taken together, we conclude that laminarin effectively promotes the growth of deep-sea *Lentisphaerae* strains WC36 and zth2, and induces the production of bacteriophages. Distinct from previous reports that bacteriophages are induced under traditional conditions such as low temperature (Wang et al., 2007), mitomycin C (Mazaheri Nezhad Fard et al., 2010), and ultraviolet irradiation (McKay and Baldwin, 1973), here, we report for the first time that polysaccharides induce the production of bacteriophages.

Bacteriophages reprogram the polysaccharide metabolism of *Lentisphaerae* strains WC36 and zth2

In this study, we clearly show that polysaccharide effectively promotes bacterial growth and simultaneously induces the production of bacteriophages, suggesting a close relationship between bacteriophages and host polysaccharide metabolism. Therefore, we sought to ask whether bacteriophages could reprogram polysaccharide metabolism in deep-sea bacteria. For this purpose, we sequenced the genomes of the bacteriophages induced by polysaccharides in *Lentisphaerae* strains WC36 and zth2. Eventually, two incomplete assembled genomes (Phage-WC36-1, 6.3 kb;

Phage-WC36-2, 28.3 kb) were obtained from the bacteriophages of strain WC36 (Figure 5A, B and Supplementary files 2, 3). Meanwhile, two incomplete assembled genomes (Phage-zth2-1, 6.3 kb; Phage-zth2-2, 40.4 kb) were obtained from the phages of strain zth2 (Figure 5A, C and Supplementary files 2, 4). Subsequently, we carefully compared the bacteriophage genomes with those of the corresponding hosts (strains WC36 and zth2) using Galaxy Version 2.6.0 (https://galaxy.pasteur.fr/) (Afgan et al., 2018) with the NCBI BLASTN method and used BWA-mem software for read mapping from host whole genome sequencing (WGS) to these bacteriophages. These analyses both showed that the bacteriophage genomes are completely outside of the host chromosomes. Through comparison of genome sequence (Figure 5—figure supplement 1), IMG database analysis, and phylogenetic analysis (Figure 5—figure supplement 2), we confirmed that Phage-WC36-1 was the same as Phage-zth2-1 (inoviruses, belonging to the family *Inoviridae*, order *Tubulavirales*, class *Faserviricetes*), indicating that inoviruses might be common in the *Lentisphaerae* phylum. Inovirus members were the dominant population in the active group of viruses from deep-sea sediments, and encode some proteins contributing to host phenotypes and ultimately alter the fitness and other behaviors of their hosts (Engelhardt et al., 2015; Mai-Prochnow et al., 2015). A maximum likelihood tree showed that both Phage-WC36-2 and Phage-zth2-2 belonged to the class *Caudoviricetes* (Figure 5—figure supplement 3). In addition to genes encoding phage-associated proteins within the assembled bacteriophage genomes, there are also many genes encoding proteins associated with polysaccharide transport and degradation, which were potential AMGs (Shaffer et al., 2020; Pratama et al., 2021). These polysaccharide metabolizing proteins include TonB-system energizer ExbB (Koebnik, 2005), O-polysaccharide acetyltransferase (Lunin et al., 2020), glucosaminidase, glycoside hydrolase family 127 protein (best BLASTP hit e-value 3e-25), and transglycosylase (Figure 5). GH127 is one of the CAZymes, which are specifically responsible for degrading polysaccharides (Cantarel et al., 2009). Energizer ExbB is an important part of the TonB-system, which is often present in *Bacteroides* and responsible for transport of oligosaccharides from the outer

membrane into the periplasm (Foley et al., 2016). It is absent in the strain WC36 and zth2 genomes, however. In natural ecosystems, viral infections indirectly influence microbial metabolic fluxes, metabolic reprogramming, and energy homeostasis of host cells (Howard-Varona et al., 2020). For example, cyanoviruses possess AMGs encoding core photosynthetic reaction centers (Sullivan et al., 2006) which are highly expressed during infection, thus stimulating photosynthesis and enhancing viral abundance (Lindell et al., 2007). Therefore, these potential AMGs encoding TonB-system energizer ExbB and glycoside hydrolases might reprogram the polysaccharide metabolism of host cells (strains WC36 and zth2) by providing supplemental support to key metabolic processes. The above results provide stronger evidence that the relationship between Phages-WC36 and their host is not a fight to the death between enemies, but in contrast a mutualistic relationship between partners (Shkoporov et al., 2022). Overall, bacteriophages induced by polysaccharides contain potential AMGs associated with polysaccharide degradation, which may play a key role in the degradation and utilization of polysaccharide by host cells.

Moreover, it was recently demonstrated that selfish bacteria, which were common throughout the water column of the ocean, could bind, partially hydrolyze, and transport polysaccharides into the periplasmic space without loss of hydrolysis products (Reintjes et al., 2017; Giljan et al., 2023). Based on our results, we hypothesized that these chronic phages might assist the host to metabolize polysaccharides in this “selfishness” mechanism, thus helping their hosts to grow and proliferate, so they could reap the benefits of simply having more hosts to infect. In addition, we found that nucleic acids could induce a deep-sea wall-less bacterium (*Hujiaoplasma nucleasis* zrk29) to release chronic bacteriophages, which might support strain zrk29 to metabolize nucleic acids without lysing host cells (Zheng et al., 2023). We also found that NO_3^- or NH_4^+ induced a deep-sea *Planctomycetes* bacterium (*Poriferisphaera heterotrophicis* ZRK32) to release a bacteriophage in a chronic manner, without host cell lysis, and this chronic phage might enable strain ZRK32 to metabolize nitrogen through the function of AMGs (Zheng et al., 2024). Therefore, the mutualism between chronic phages and hosts may

be widespread in the deep-sea microbes. However, it is difficult to conduct more experiments to prove the mechanistic roles of the AMGs in promoting both host and phage proliferation in these strictly anaerobic deep-sea microbes. In the future, we need to construct genetic operating systems of these strictly anaerobic host strains to reveal the relationship between chronic phage and host.

Materials and methods

Samples, media, and cultivation conditions

Deep-sea samples used for bacteria isolation in this study were collected from a typical cold seep (E119º17'07.322", N22º06'58.598") at a depth of 1146 m by *RV KEXUE* in July of 2018. Inorganic medium (including 1.0 g/L NH_4Cl, 1.0 g/L $NaHCO_3$, 1.0 g/L CH_3COONa, 0.5 g/L KH_2PO_4, 0.2 g/L $MgSO_4 \cdot 7H_2O$, 0.7 g/L cysteine hydrochloride, 500 µl/L 0.1 % (w/v) resazurin, 1 L filtered seawater, pH 7.0) supplemented with 1.0 g/L of different polysaccharides (laminarin, fucoidan, starch, and alginate) under a 100% N_2 atmosphere was used to enrich microbes at 28 °C for one month (Zheng et al., 2021a). The detailed isolation and purification steps were performed as described previously (Zheng et al., 2021b). After pure cultures of deep-sea bacteria were obtained, we cultured them in a rich medium (containing 1.0 g/L peptone, 5.0 g/L yeast extract, 1.0 g/L NH_4Cl, 1.0 g/L $NaHCO_3$, 1.0 g/L CH_3COONa, 0.5 g/L KH_2PO_4, 0.2 g/L $MgSO_4 \cdot 7H_2O$, 0.7 g/L cysteine hydrochloride, 500 µl/L 0.1 % (w/v) resazurin, 1 L filtered seawater, pH 7.0) or rich medium supplemented with different polysaccharides for the future research.

Genome sequencing, annotation, and analysis of strains WC36 and zth2

For genomic sequencing, strains WC36 and zth2 were grown in the liquid rich medium supplemented with 5 g/L laminarin and starch and harvested after one week of incubation at 28 °C. Genomic DNA was isolated by using the PowerSoil DNA isolation kit (Mo Bio Laboratories Inc., Carlsbad, CA). Thereafter, the genome sequencing was carried out with both the Illumina NovaSeq PE150 (San Diego, USA) and Nanopore PromethION platform (Oxford, UK) at the Beijing Novogene

Bioinformatics Technology Co., Ltd. A complete description of the library construction, sequencing, and assembly was performed as previously described (Zheng et al., 2021b). We used seven databases to predict gene functions, including Pfam (Protein Families Database, http://pfam.xfam.org/), GO (Gene Ontology, http://geneontology.org/) (Ashburner et al., 2000), KEGG (Kyoto Encyclopedia of Genes and Genomes, http://www.genome.jp/kegg/) (Kanehisa et al., 2004), COG (Clusters of Orthologous Groups, http://www.ncbi.nlm.nih.gov/COG/) (Galperin et al., 2015), NR (Non-Redundant Protein Database databases), TCDB (Transporter Classification Database), and Swiss-Prot (http://www.ebi.ac.uk/uniprot/) (Bairoch and Apweiler, 2000). A whole genome Blast search (E-value less than 1e-5, minimal alignment length percentage larger than 40%) was performed against above seven databases.

Phylogenetic analysis

The 16S rRNA gene tree was constructed based on full-length 16S rRNA gene sequences by the maximum likelihood method. The full-length 16S rRNA gene sequences of *Lentisphaerae* strains WC36 and zth2 were obtained from their genomes, and the 16S rRNA gene sequences of other related taxa used for phylogenetic analysis were obtained from NCBI (www.ncbi.nlm.nih.gov/). All the accession numbers were listed in the Supplementary file 5. The maximum likelihood phylogenetic trees of Phage-WC36-1 were constructed based on the zona occludens toxin (Zot) and single-stranded DNA-binding protein (Zeng et al., 2021; Evseev et al., 2023). The maximum likelihood phylogenetic tree of Phage-WC36-2 and Phage-zth2-2 was constructed based on the terminase large subunit protein (*terL*). These proteins used to construct the phylogenetic trees were all obtained from the NCBI databases. All the sequences were aligned by MAFFT version 7 (Katoh et al., 2019) and manually corrected. The phylogenetic trees were constructed using the W-IQ-TREE web server (http://iqtree.cibiv.univie.ac.at) with the “GTR+F+I+G4” model (Trifinopoulos et al., 2016). Finally, we used the online tool Interactive Tree of Life (iTOL v5) (Letunic and Bork, 2021) to edit the tree.

Growth assay and transcriptomic analysis of *Lentisphaerae* strains WC36 and zth2 cultured in medium supplemented with laminarin

To assess the effect of polysaccharide on the growth of strain WC36, 100 µl of freshly incubated cells were inoculated in a 15 mL Hungate tube containing 10 mL rich medium supplemented with or without 5 g/L or 10 g/L laminarin (or starch). To assess the effect of laminarin on the growth of strain zth2, 100 µL of freshly incubated cells were inoculated in a 15 mL Hungate tube containing 10 mL rich medium supplemented with or without 3 g/L laminarin. Each condition was performed in three replicates. All the Hungate tubes were incubated at 28 °C. The bacterial growth status was monitored by measuring the OD_{600} value via a microplate reader (Infinite M1000 Pro; Tecan, Mannedorf, Switzerland) every day until cell growth reached the stationary phase.

For transcriptomic analysis, a cell suspension of strain WC36 was harvested after culture in 1.5 L rich medium either without supplementation or with 10 g/L laminarin for 5 days and 10 days. A cell suspension of strain zth2 was harvested after culture in rich medium either without supplementation or with 3 g/L laminarin for 4 days. Thereafter, these collected samples were used for transcriptomic analysis by Novogene (Tianjin, China). The detailed procedures of the transcriptomic assays including library preparation, clustering, and sequencing, and data analyses are described in the supplementary information.

Bacteriophages isolation

Phage isolation was as described previously with some modifications (Yamamoto et al., 1970; Tseng et al., 1990; Kim and Blaschek, 1991). To induce the production of bacteriophages, strain WC36 was inoculated in rich medium supplemented with or without 10 g/L laminarin or 10 g/L starch, and strain zth2 was cultured in rich medium supplemented with or without 3 g/L laminarin or 3 g/L starch. After 10 days incubation, 60 mL of the different cultures was respectively collected and cells were removed by centrifugation at 8,000 × *g*, 4 °C for 20 minutes three times. The supernatant was filtered through a 0.22 µm millipore filter (Pall Supor, New York,

America) and subsequently 1 M NaCl was added to lyse the bacteria and separate phage particles from these bacterial fragments. Then the supernatant was filtered through a 0.22 μm millipore filter and collected by centrifugation at 8,000 × *g*, 4 °C for 20 minutes, and phage particles were immediately precipitated with 100 g/L polyethylene glycol (PEG8000) at 4 °C for 6 hours, and collected by centrifugation at 10,000 × *g*, 4 °C for 20 minutes. The resulting phage particles were suspended in 2 mL SM buffer (0.01% gelatin, 50 mM Tris-HCl, 100 mM NaCl, and 10 mM $MgSO_4$), then the suspension was extracted three times with an equal volume of chloroform (Lin et al., 2012) and collected by centrifugation at 4,000 × *g*, 4 °C for 20 minutes. Finally, clean phage particles were obtained.

Transmission electron microscopy (TEM)

To observe the morphology of bacteriophages, 10 μL phage virions were allowed to adsorb onto a copper grid for 20 minutes, and then stained with phosphotungstic acid for 30 seconds. Next, micrographs were taken with TEM (HT7700, Hitachi, Japan) with a JEOL JEM 12000 EX (equipped with a field emission gun) at 100 kV.

To observe the morphology of strain WC36, cell suspension in rich medium supplemented with or without polysaccharide was centrifuged at 5,000 × *g* for 10 minutes to obtain cell pellets. Subsequently, one part of the cell collection was adsorbed to the copper grids for 20 minutes, then washed with 10 mM phosphate buffer solution (PBS, pH 7.4) for 10 minutes and dried at room temperature for TEM observation. Another part was first preserved in 2.5% glutaraldehyde for 24 hours at 4 °C, and then washed three times with PBS and dehydrated in ethanol solutions of 30%, 50%, 70%, 90%, and 100% for 10 minutes each time. Samples were further fixed in 1% osmium tetroxide for 2 hours and embedded in plastic resin (Zechmann and Zellnig, 2009; Fortunato et al., 2016). Thereafter, an ultramicrotome (Leica EM UC7, Germany) was used to prepare ultrathin sections (50 nm) of cells, and the obtained sections were stained with uranyl acetate and lead citrate (Graham and Orenstein, 2007; Panphut et al., 2011). Finally, all samples were observed with the JEOL JEM-1200 electron microscope as described above. In parallel, the phage'

number in each condition was respectively calculated by ten random TEM images.

Genome sequencing of bacteriophages

To sequence the genomes of bacteriophages, phage genomic DNA was extracted from different purified phage particles. Briefly, 1 μg/mL DNase I and RNase A were added to the concentrated phage solution for nucleic acid digestion overnight at 37 °C. The digestion treatment was inactivated at 80 °C for 15 minutes, followed by extraction with a Viral DNA Kit (Omega Bio-tek, USA) according to the manufacturer's instructions. Then, genome sequencing was performed by Biozeron Biological Technology Co. Ltd (Shanghai, China). The detailed process of library construction, sequencing, genome assembly and annotation is described in the supplementary information. In order to detect whether these bacteriophage genomes were located within or outside of the host chromosomes, we used the new alignment algorithm BWA-MEM (version 0.7.15) (Li, 2013) with default parameters to perform read mapping of host WGS to these phages. In addition, we also evaluated the assembly graph underlying the host consensus assemblies. Clean reads were mapped to the bacterial complete genome sequences by Bowtie 2 (version 2.5.0) (Langmead and Salzberg, 2012), BWA (version 0.7.8) (Li and Durbin, 2009), and SAMTOOLS (version 0.1.18) (Li et al., 2009) with the default parameters.

Data availability

The complete genome sequences of strains WC36 and zth2 presented in this study have been deposited in the GenBank database with accession numbers CP085689 and CP071032, respectively. The whole 16S rRNA gene sequences of strains WC36 and zth2 have been deposited in the GenBank database with accession numbers OK614042 and MW729759, respectively. The genome sequences of Phage-WC36-1 (Phage-zth2-1), Phage-WC36-2, and Phage-zth2-2 have been deposited in the GenBank database with accession numbers PP701473, OL791266, and OL791268, respectively. The raw sequencing reads from the transcriptomics analysis have been deposited to the NCBI Short Read Archive (accession numbers: PRJNA946146,

PRJNA756144, and PRJNA865570).

Acknowledgements

This work was funded by the Science and Technology Innovation Project of Laoshan Laboratory (Grant no. 2022QNLM030004-3 and LSKJ202203103), the NSFC Innovative Group Grant (No. 42221005), Major Research Plan of the National Natural Science Foundation (Grant no. 92351301), Shandong Provincial Natural Science Foundation (ZR2021ZD28 and ZR2023QD010), Strategic Priority Research Program of the Chinese Academy of Sciences (Grant no. XDA22050301), Key Collaborative Research Program of the Alliance of International Science Organizations (Grant no. ANSO-CR-KP-2022-08), and the Taishan Scholars Program (Grant nos. tstp20230637 and tsqn202312264).

Conflict of interest

The authors declare no competing interests.

References

Ackermann, H.W. (2007) **5500 Phages examined in the electron microscope** *Arch Virol* **152**:227-243

Ackermann, H.W. (2009) **Phage classification and characterization** *Methods Mol Biol* **501**:127-140

Afgan, E., Baker, D., Batut, B., van den Beek, M., Bouvier, D., Cech, M., Chilton, J., Clements, D., Coraor, N., Grüning, B.A., et al. (2018) **The Galaxy platform for accessible, reproducible and collaborative biomedical analyses: 2018 update** *Nucleic Acids Res* **46**:W537-W544

Ahlgren, N.A., Fuchsman, C.A., Rocap, G., and Fuhrman, J.A. (2019) **Discovery of several novel, widespread, and ecologically distinct marine *Thaumarchaeota* viruses that encode *amoC* nitrification genes** *ISME J* **13**:618-631

Alarcón-Schumacher, T., Naor, A., Gophna, U., and Erdmann, S. (2022) **Isolation of a virus causing a chronic infection in the archaeal model organism *Haloferax volcanii* reveals antiviral activities of a provirus** *Proc Natl Acad Sci USA* **119**:e2205037119

Anantharaman, K., Duhaime, M.B., Breier, J.A., Wendt, K.A., Toner, B.M., and Dick, G.J. (2014) **Sulfur oxidation genes in diverse deep-sea viruses** *Science* **344**:757-760

Ashburner, M., Ball, C.A., Blake, J.A., Botstein, D., Butler, H., Cherry, J.M., Davis, A.P., Dolinski, K., Dwight, S.S., Eppig, J.T., et al. (2000) **Gene ontology: tool for the unification of biology. The Gene Ontology Consortium** *Nat Genet* **25**:25-29

Bairoch, A., and Apweiler, R. (2000) **The SWISS-PROT protein sequence database and its supplement TrEMBL in 2000** *Nucleic Acids Res* **28**:45-48

Bille, E., Zahar, J.R., Perrin, A., Morelle, S., Kriz, P., Jolley, K.A., Maiden, M.C., Dervin, C., Nassif, X., and Tinsley, C.R. (2005) **A chromosomally integrated bacteriophage in invasive meningococci** *J Exp Med* **201**:1905-1913

Breitbart, M. (2012) **Marine viruses: truth or dare** *Ann Rev Mar Sci* **4**:425-448

Brum, J.R., and Sullivan, M.B. (2015) **Rising to the challenge: accelerated pace of discovery transforms marine virology** *Nat Rev Microbiol* **13**:147-159

Brum, J.R., Ignacio-Espinoza, J.C., Kim, E.H., Trubl, G., Jones, R.M., Roux, S., VerBerkmoes, N.C., Rich, V.I., and Sullivan, M.B. (2016) **Illuminating structural proteins in viral "dark matter" with metaproteomics** *Proc Natl Acad Sci USA* **113**:2436-2441

Cantarel, B.L., Coutinho, P.M., Rancurel, C., Bernard, T., Lombard, V., and Henrissat, B. (2009) **The Carbohydrate-Active EnZymes database (CAZy): an expert resource for Glycogenomics** *Nucleic Acids Res* **37**:D233-238

Chevallereau, A., Pons, B.J., van Houte, S., and Westra, E.R. (2022) **Interactions between bacterial and phage communities in natural environments** *Nat Rev Microbiol* **20**:49-62

Davis, B.M., Lawson, E.H., Sandkvist, M., Ali, A., Sozhamannan, S., and Waldor, M.K. (2000) **Convergence of the secretory pathways for cholera toxin and the filamentous phage, CTXphi** *Science* **288**:333-335

Dominguez-Huerta, G., Zayed, A.A., Wainaina, J.M., Guo, J., Tian, F., Pratama, A.A., Bolduc, B., Mohssen, M., Zablocki, O., Pelletier, E., et al. (2022) **Diversity and ecological footprint of Global Ocean RNA viruses** *Science* **376**:1202-1208

Du Toit, A. (2017) **Viral infection: The language of phages** *Nat Rev Microbiol* **15**:134-135

Dwivedi, B., Xue, B., Lundin, D., Edwards, R.A., and Breitbart, M. (2013) **A bioinformatic analysis of ribonucleotide reductase genes in phage genomes and metagenomes** *BMC Evol Biol* **13**:33

Enav, H., Mandel-Gutfreund, Y., and Béjà, O. (2014) **Comparative metagenomic analyses reveal viral-induced shifts of host metabolism towards nucleotide biosynthesis** *Microbiome* **2**:9

Engelhardt, T., Orsi, W.D., and Jørgensen, B.B. (2015) **Viral activities and life cycles in deep subseafloor sediments** *Environ Microbiol Rep* **7**:868-873

Evseev, P., Bocharova, J., Shagin, D., and Chebotar, I. (2023) **Analysis of *Pseudomonas aeruginosa* isolates from patients with cystic fibrosis revealed novel groups of filamentous bacteriophages** *Viruses* **15**:2215

Falkowski, P.G., Barber, R.T., and Smetacek, V. (1998) **Biogeochemical controls and feedbacks on ocean primary production** *Science* **281**:200-206

Faust, K., and Raes, J. (2012) **Microbial interactions: from networks to models** *Nat Rev Microbiol* **10**:538-550

Foley, M.H., Cockburn, D.W., and Koropatkin, N.M. (2016) **The Sus operon: a model system for starch uptake by the human gut *Bacteroidetes*** *Cell Mol Life Sci* **73**:2603-2617

Fortunato, T.M., Beltrami, C., Emanueli, C., De Bank, P.A., and Pula, G. (2016) **Platelet lysate gel and endothelial progenitors stimulate microvascular network formation in vitro: tissue engineering implications** *Sci Rep* **6**:25326

Galperin, M.Y., Makarova, K.S., Wolf, Y.I., and Koonin, E.V. (2015) **Expanded microbial genome coverage and improved protein family annotation in the COG database** *Nucleic Acids Res* **43**:D261-269

Gazitúa, M.C., Vik, D.R., Roux, S., Gregory, A.C., Bolduc, B., Widner, B., Mulholland, M.R., Hallam, S.J., Ulloa, O., and Sullivan, M.B. (2021) **Potential virus-mediated nitrogen cycling in oxygen-depleted oceanic waters** *ISME J* **15**:981-998

Giljan, G., Brown, S., Lloyd, C.C., Ghobrial, S., Amann, R., and Arnosti, C. (2023) **Selfish bacteria are active throughout the water column of the ocean** *ISME Commun* **3**:11

Godkin, A., and Smith, K.A. (2017) **Chronic infections with viruses or parasites: breaking bad to make good** *Immunology* **150**:389-396

Graham, L., and Orenstein, J.M. (2007) **Processing tissue and cells for transmission electron microscopy in diagnostic pathology and research** *Nat Protoc* **2**:2439-2450

Gregory, A.C., Zayed, A.A., Conceição-Neto, N., Temperton, B., Bolduc, B., Alberti, A., Ardyna, M., Arkhipova, K., Carmichael, M., Cruaud, C., et al. (2019) **Marine DNA Viral Macro- and Microdiversity from Pole to Pole** *Cell* **177**:1109-1123.e1114

Hoffmann Berling, H., and Maze, R. (1964) **Release of male-specific bacteriophages from surviving host bacteria** *Virology* **22**:305-313

Howard-Varona, C., Hargreaves, K.R., Abedon, S.T., and Sullivan, M.B. (2017) **Lysogeny in nature: mechanisms, impact and ecology of temperate phages** *ISME J* **11**:1511-1520

Howard-Varona, C., Lindback, M.M., Bastien, G.E., Solonenko, N., Zayed, A.A., Jang, H., Andreopoulos, B., Brewer, H.M., del Rio, T.G., Adkins, J.N., et al. (2020) **Phage-specific metabolic reprogramming of virocells** *ISME J* **14**:881-895

Hurwitz, B.L., Hallam, S.J., and Sullivan, M.B. (2013) **Metabolic reprogramming by viruses in the sunlit and dark ocean** *Genome Biol* **14**:R123

Jiang, S.C., and Paul, J.H. (1996) **Occurrence of lysogenic bacteria in marine microbial communities as determined by prophage induction** *Mar Ecol Prog Ser* **142**:27-38

Kanehisa, M., Goto, S., Kawashima, S., Okuno, Y., and Hattori, M. (2004) **The KEGG resource for deciphering the genome** *Nucleic Acids Res* **32**:D277-280

Katoh, K., Rozewicki, J., and Yamada, K.D. (2019) **MAFFT online service: multiple sequence alignment, interactive sequence choice and visualization** *Brief Bioinform* **20**:1160-1166

Kim, A.Y., and Blaschek, H.P. (1991) **Isolation and characterization of a filamentous viruslike particle from *Clostridium acetobutylicum* NCIB 6444** *J Bacteriol* **173**:530-535

Knezevic, P., Adriaenssens, E.M., and Ictv Report, C. (2021) **ICTV Virus Taxonomy Profile: Inoviridae** *J Gen Virol* **102**:

Koebnik, R. (2005) **TonB-dependent trans-envelope signalling: the exception or the rule?** *Trends Microbiol* **13**:343-347

Krupovic, M., and Consortium, I.R. (2018) **ICTV virus taxonomy profile: *Plasmaviridae*** *J Gen Virol* **99**:617-618

Langmead, B., and Salzberg, S.L. (2012) **Fast gapped-read alignment with Bowtie 2** *Nat Methods* **9**:357-359

Letunic, I., and Bork, P. (2021) **Interactive Tree Of Life (iTOL) v5: an online tool for phylogenetic tree display and annotation** *Nucleic Acids Res* **49**:W293-W296

Li, H. (2013) **Aligning sequence reads, clone sequences and assembly contigs with BWA-MEM** *ArXiv* preprint arXiv:1303.3997

Li, H., and Durbin, R. (2009) **Fast and accurate short read alignment with Burrows-Wheeler transform** *Bioinformatics* **25**:1754-1760

Li, H., Handsaker, B., Wysoker, A., Fennell, T., Ruan, J., Homer, N., Marth, G., Abecasis, G., and Durbin, R. (2009) **The Sequence Alignment/Map format and SAMtools** *Bioinformatics* **25**:2078-2079

Li, Z., Pan, D., Wei, G., Pi, W., Zhang, C., Wang, J.H., Peng, Y., Zhang, L., Wang, Y., Hubert, C.R.J., et al. (2021) **Deep sea sediments associated with cold seeps are a subsurface reservoir of viral diversity** *ISME J* **15**:2366-2378

Lin, Y.R., Chiu, C.W., Chang, F.Y., and Lin, C.S. (2012) **Characterization of a new phage, termed phi A318, which is specific for *Vibrio alginolyticus*** *Arch Virol* **157**:917-926

Lindell, D., Jaffe, J.D., Coleman, M.L., Futschik, M.E., Axmann, I.M., Rector, T., Kettler, G., Sullivan, M.B., Steen, R., Hess, W.R., et al. (2007) **Genome-wide expression dynamics of a marine virus and host reveal features of co-evolution** *Nature* **449**:83-86

Liu, Y., Alexeeva, S., Bachmann, H., Guerra Martínez, J.A., Yeremenko, N., Abee, T., and Smid, E.J. (2022) **Chronic release of tailless phage particles from *Lactococcus lactis*** *Appl Environ Microbiol* **88**:e0148321

Lunin, V.V., Wang, H.-T., Bharadwaj, V.S., Alahuhta, M., Peña, M.J., Yang, J.-Y., Archer-Hartmann, S.A., Azadi, P., Himmel, M.E., Moremen, K.W., et al. (2020) **Molecular mechanism of polysaccharide acetylation by the arabidopsis xylan O-acetyltransferase XOAT1** *Plant Cell* **32**:2367-2382

Mäntynen, S., Laanto, E., Oksanen, H.M., Poranen, M.M., and Díaz-Muñoz, S.L. (2021) **Black box of phage-bacterium interactions: exploring alternative phage infection strategies** *Open Biol* **11**:210188

Mai-Prochnow, A., Hui, J.G., Kjelleberg, S., Rakonjac, J., McDougald, D., and Rice, S.A. (2015) **'Big things in small packages: the genetics of filamentous phage and effects on fitness of their host'** *FEMS Microbiol Rev* **39**:465-487

Mann, N.H., Cook, A., Millard, A., Bailey, S., and Clokie, M. (2003) **Marine ecosystems: bacterial photosynthesis genes in a virus** *Nature* **424**:741

Marvin, D.A., Symmons, M.F., and Straus, S.K. (2014) **Structure and assembly of filamentous bacteriophages** *Prog Biophys Mol Bio* **114**:80-122

Mazaheri Nezhad Fard, R., Barton, M.D., and Heuzenroeder, M.W. (2010) **Novel bacteriophages in *Enterococcus* spp** *Curr Microbiol* **60**:400-406

McKay, L.L., and Baldwin, K.A. (1973) **Induction of prophage in *Streptococcus lactis* C2 by ultraviolet irradiation** *Appl Microbiol* **25**:682-684

Panphut, W., Senapin, S., Sriurairatana, S., Withyachumnarnkul, B., and Flegel, T.W. (2011) **A novel integrase-containing element may interact with Laem-Singh virus (LSNV) to cause slow growth in giant tiger shrimp** *BMC Vet Res* **7**:18

Pratama, A.A., Bolduc, B., Zayed, A.A., Zhong, Z.P., Guo, J., Vik, D.R., Gazitúa, M.C., Wainaina, J.M., Roux, S., and Sullivan, M.B. (2021) **Expanding standards in viromics: in silico evaluation of dsDNA viral genome identification, classification, and auxiliary metabolic gene curation** *PeerJ* **9**:e11447

Putzrath, R.M., and Maniloff, J. (1977) **Growth of an enveloped mycoplasmavirus and establishment of a carrier state** *J Virol* **22**:308-314

Reintjes, G., Arnosti, C., Fuchs, B.M., and Amann, R. (2017) **An alternative polysaccharide uptake mechanism of marine bacteria** *ISME J* **11**:1640-1650

Roux, S., Krupovic, M., Daly, R.A., Borges, A.L., Nayfach, S., Schulz, F., Sharrar, A., Matheus Carnevali, P.B., Cheng, J.F., Ivanova, N.N., et al. (2019) **Cryptic inoviruses revealed as pervasive in bacteria and archaea across Earth's biomes** *Nat Microbiol* **4**:1895-1906

Roux, S., Brum, J.R., Dutilh, B.E., Sunagawa, S., Duhaime, M.B., Loy, A., Poulos, B.T., Solonenko, N., Lara, E., Poulain, J., et al. (2016) **Ecogenomics and potential biogeochemical impacts of globally abundant ocean viruses** *Nature* **537**:689-693

Russel, M. (1991) **Filamentous phage assembly** *Mol Microbiol* **5**:1607-1613

Samson, J.E., Magadán, A.H., Sabri, M., and Moineau, S. (2013) **Revenge of the phages: defeating bacterial defences** *Nat Rev Microbiol* **11**:675-687

Shaffer, M., Borton, M.A., McGivern, B.B., Zayed, A.A., La Rosa, S.L., Solden, L.M., Liu, P., Narrowe, A.B., Rodríguez-Ramos, J., Bolduc, B., et al. (2020) **DRAM for distilling microbial metabolism to automate the curation of microbiome function** *Nucleic Acids Res* **48**:8883-8900

Shkoporov, A.N., Turkington, C.J., and Hill, C. (2022) **Mutualistic interplay between bacteriophages and bacteria in the human gut** *Nat Rev Microbiol*

Sullivan, M.B., Coleman, M.L., Weigele, P., Rohwer, F., and Chisholm, S.W. (2005) **Three *Prochlorococcus* cyanophage genomes: signature features and ecological interpretations** *PLoS Biol* **3**:e144

Sullivan, M.B., Lindell, D., Lee, J.A., Thompson, L.R., Bielawski, J.P., and Chisholm, S.W. (2006) **Prevalence and evolution of core photosystem II genes in marine cyanobacterial viruses and their hosts** *PLoS Biol* **4**:e234

Suttle, C.A. (2005) **Viruses in the sea** *Nature* **437**:356-361

Suttle, C.A. (2007) **Marine viruses--major players in the global ecosystem** *Nat Rev Microbiol* **5**:801-812

Trifinopoulos, J., Nguyen, L.T., von Haeseler, A., and Minh, B.Q. (2016) **W-IQ-TREE: a fast online phylogenetic tool for maximum likelihood analysis** *Nucleic Acids Res* **44**:W232-W235

Tseng, Y.H., Lo, M.C., Lin, K.C., Pan, C.C., and Chang, R.Y. (1990) **Characterization of filamentous bacteriophage phi Lf from *Xanthomonas campestris* pv. campestris** *J Gen Virol* **71(Pt8)**:1881-1884

Wang, F., Wang, F., Li, Q., and Xiao, X. (2007) **A novel filamentous phage from the deep-sea bacterium *Shewanella piezotolerans* WP3 is induced at low temperature** *J Bacteriol* **189**:7151-7153

Weinbauer, M.G., Wilhelm, S.W., and Suttle, C.A. (1999) **Sunlight-lnduced DNA damage and resistance in natural viral communities** *Aquat Microb Ecol* **17**:111-120

Wigington, C.H., Sonderegger, D., Brussaard, C.P., Buchan, A., Finke, J.F., Fuhrman, J.A., Lennon, J.T., Middelboe, M., Suttle, C.A., Stock, C., et al. (2016) **Re-examination of the relationship between marine virus and microbial cell abundances** *Nat Microbiol* **1**:15024

Yamamoto, K.R., Alberts, B.M., Benzinger, R., Lawhorne, L., and Treiber, G. (1970) **Rapid bacteriophage sedimentation in the presence of polyethylene glycol and its application to large-scale virus purification** *Virology* **40**:734-744

Yarza, P., Yilmaz, P., Pruesse, E., Glöckner, F.O., Ludwig, W., Schleifer, K.H., Whitman, W.B., Euzéby, J., Amann, R., and Rosselló-Móra, R. (2014) **Uniting the classification of cultured and uncultured bacteria and archaea using 16S rRNA gene sequences** *Nat Rev Microbiol* **12**:635-645

Zechmann, B., and Zellnig, G. (2009) **Rapid diagnosis of plant virus diseases by transmission electron microscopy** *J Virol Methods* **162**:163-169

Zeng, J., Wang, Y., Zhang, J., Yang, S., and Zhang, W. (2021) **Multiple novel filamentous phages detected in the cloacal swab samples of birds using viral metagenomics approach** *Virol J* **18**:240

Zeng, Q., and Chisholm, S.W. (2012) **Marine viruses exploit their host's two-component regulatory system in response to resource limitation** *Curr Biol* **22**:124-128

Zhang, T., Zheng, R., Liu, R., Li, R., and Sun, C. (2022) **Cultivation and functional characterization of a deep-sea *Lentisphaerae* representative reveals its unique physiology and ecology** *Front Mar Sci* **9**:848136

Zheng, R., Cai, R., Liu, R., Liu, G., and Sun, C. (2021a) ***Maribellus comscasis* sp. nov., a novel deep-sea *Bacteroidetes* bacterium, possessing a prominent capability of degrading cellulose** *Environ Microbiol* **23**:4561-4575

Zheng, R., Wang, C., Cai, R., Shan, Y., and Sun, C. (2023) **Mechanisms of nucleic acid degradation and high hydrostatic pressure tolerance of a novel deep-sea wall-less bacterium** *mBio* **14**:e0095823

Zheng, R., Wang, C., Liu, R., Cai, R., and Sun, C. (2024) **Physiological and metabolic insights into the first cultured anaerobic representative of deep-sea *Planctomycetes* bacteria** *Elife* **12**:RP89874

Zheng, R., Liu, R., Shan, Y., Cai, R., Liu, G., and Sun, C. (2021b) **Characterization of the first cultured free-living representative of *Candidatus* Izemoplasma uncovers its unique biology** *ISME J* **15**:2676-2691

Zimmerman, A.E., Howard-Varona, C., Needham, D.M., John, S.G., Worden, A.Z., Sullivan, M.B., Waldbauer, J.R., and Coleman, M.L. (2020) **Metabolic and biogeochemical consequences of viral infection in aquatic ecosystems** *Nat Rev Microbiol* **18**:21-34

Figure Legends

Figure 1. Polysaccharides promote the deep-sea *Lentisphaerae* strain WC36 growth and stimulate the expression of phage-associated genes. (A) Maximum likelihood phylogenetic tree of 16S rRNA gene sequences from strain WC36, strain zth2, and some *Planctomycetes-Verrucomicrobia-Chlamydia* (PVC) group bacteria. *Bacillus cereus* ATCC 14579 was used as the outgroup. Bootstrap values (%) > 80 are indicated at the base of each node with the gray dots (expressed as percentages of 1000 replications). The accession number is displayed behind corresponding strain. (B) Growth assays of strain WC36 cultivated in rich medium either without supplementation, with 5 g/L or 10 g/L laminarin or with 5 g/L or 10 g/L starch. (C) Transcriptomics-based heat map showing all up-regulated genes encoding phage-associated proteins in strain WC36 cultured in rich medium supplemented with 10 g/L laminarin. “Rich” indicates strain WC36 cultivated in rich medium; “Lam” indicates strain WC36 cultivated in rich medium supplemented with 10 g/L laminarin. (D) RT-qPCR detection of the expression of some genes encoding phage-associated proteins shown in panel C. The heat map was generated by Heml 1.0.3.3. The numbers in panel C represent multiple differences in gene expression (by taking $\log_2$ values).

Figure 2. Polysaccharides induce the production of bacteriophages in *Lentisphaerae* strain WC36. (A) TEM observation of phages extracted from the supernatant of WC36 cells cultured in rich medium supplemented with or without polysaccharide. Panel I shows the absence of phages in the supernatant of WC36 cells cultivated in rich medium. Panels II-IV show the morphology of phages present in the supernatant of WC36 cells cultivated in rich medium supplemented with 10 g/L laminarin. Yellow hollow arrows indicate the typical granular structure of filamentous phages, and green arrows indicate phage-like particles with other shapes. Panels V-VIII show the morphology of phages present in the supernatant of strain WC36 cells cultivated in rich medium supplemented with 10 g/L starch. Typical filamentous phages are indicated with yellow hollow arrows, and two other kinds of phage-like particles with different shapes are indicated by orange and green arrows, respectively.

(B) TEM observation of strain WC36 cultured in rich medium supplemented with or without 10 g/L laminarin or 10 g/L starch. Panel I shows representative morphology of strain WC36 cultivated in rich medium. Panel II shows the morphology of strain WC36 cultivated in rich medium supplemented with 10 g/L laminarin. Panels III-IV show the morphology of strain WC36 cultivated in rich medium supplemented with 10 g/L starch. Red arrows indicate filamentous phages associated with bacterial cells. (C) TEM of an ultrathin section of strain WC36 cultured in rich medium supplemented with or without 10 g/L laminarin or 10 g/L starch. Panel I shows an ultrathin section of strain WC36 cultivated in rich medium; Panels II-III show ultrathin sections of strain WC36 cultivated in rich medium supplemented with 10 g/L laminarin; Panel IV shows an observation of the ultrathin section of strain WC36 cultivated in rich medium supplemented with 10 g/L starch. Red arrows indicate filamentous phages being released from or entering bacterial cells.

Figure 2—figure supplement 1. TEM observation of potential phage-like particles extracted from the rich medium supplemented with 10 g/L laminarin alone (A) or 10 g/L starch alone (B).

Figure 2—figure supplement 2. TEM observation of the rich medium supplemented with 10 g/L laminarin alone (A) or 10 g/L starch alone (B).

Figure 2—figure supplement 3. The morphology of *Lentisphaerae* strain WC36 and its released filamentous bacteriophages. (A) TEM observation of the morphology of released filamentous bacteriophages and strain WC36 cultured in rich medium supplemented without (panels I-III) or with (panels IV-VI) 10 g/L laminarin for 5, 10, and 30 days, respectively. “Lam” indicate the potential laminarin adhered to bacterial cells. The filamentous phages released from bacterial cells were pointed using red arrows. (B) TEM observation of an ultrathin section of strain WC36 cultured in rich medium supplemented without (panel I) or with (panels II-III) 10 g/L laminarin. White arrows indicate the extrusions or buddings around bacterial cells.

Figure 3. Bacteriophages induced from *Lentisphaerae* strain WC36 by polysaccharides are released via chronic manners. (A) Growth curve of strain WC36 cultivated in either rich medium alone or rich medium supplemented with 5 g/L or 10 g/L laminarin for 30 days. The number of filamentous phages (B) and

hexagonal phages (C) extracted from 1 μL of the supernatant of strain WC36 cell cultured in rich medium supplemented with or without 5 g/L or 10 g/L laminarin (for 5, 10, and 30 days). The average numbers are shown at the top of the bar charts.

Figure 3—figure supplement 1. TEM observation of filamentous phages extracted from the supernatant of strain WC36 cell suspension cultured in rich medium supplemented with or without 5 g/L or 10 g/L laminarin (for 5, 10, and 30 days). Panels I-III show the absence of phages in the supernatant of cell strain WC36 cultivated in rich medium for 5, 10, and 30 days, respectively. Panels IV-VI show the morphology of filamentous phages present in the supernatant of cell strain WC36 cultivated in rich medium supplemented with 5 g/L laminarin for 5, 10, and 30 days, respectively. Panels VII-IX show the morphology of filamentous phages present in the supernatant of cell strain WC36 cultivated in rich medium supplemented with 10 g/L laminarin for 5, 10, and 30 days, respectively. Scale bars, 1 μm.

Figure 4. Polysaccharides promote the growth of deep-sea *Lentisphaerae* strain zth2 and induce the production of bacteriophages. (A) Growth assays of strain zth2 cultivated in rich medium supplemented with or without 3 g/L laminarin for four days. (B) Transcriptomics-based heat map showing all up-regulated genes encoding phage-associated proteins in strain zth2 cultured in rich medium supplemented with 3 g/L laminarin. (C) RT-qPCR detection of the expressions of some genes encoding phage-associated proteins shown in panel B. The numbers in panel C represent multiple differences in gene expression (by taking $\log_2$ values). (D) TEM observation of phages extracted from the supernatant of a cell suspension of strain zth2 cultured in the rich medium supplemented with or without polysaccharides. Panels I-III show the morphology of phages in the cell supernatant of strain zth2 cultivated in rich medium supplemented with 3 g/L laminarin. Typical filamentous phage is indicated with yellow hollow arrows, and two other kinds of phage-like particles with different shapes are indicated by orange and green arrows, respectively. Panels IV-V show the morphology of phages present in the cell supernatant of strain zth2 cultivated in rich medium supplemented with 3 g/L starch. Typical filamentous phages are indicated with red arrows, and other phage-like particles with different shapes are indicated by

green arrows. Panel VI shows that no phages were observed in the cell supernatant of strain zth2 cultivated in rich medium. “Rich” indicates strain zth2 cultivated in rich medium; “Lam” indicates strain zth2 cultivated in rich medium supplemented with 3 g/L laminarin.

Figure 4—figure supplement 1. Transcriptome profiles and RT-qPCR analysis of the genes encoding secretion system related proteins. (A) Transcriptomics-based heat map showing all up-regulated genes encoding secretion system-associated proteins in *Lentisphaerae* strain WC36. “Rich” indicates strain WC36 cultivated in rich medium; “Lam” indicates strain WC36 cultivated in rich medium supplemented with 10 g/L laminarin. (B) RT-qPCR detection of the expression of genes shown in panel A. (C) Transcriptomics-based heat map showing all up-regulated genes encoding secretion system-associated proteins in strain zth2. “Rich” indicates strain zth2 cultivated in rich medium; “Lam” indicates strain zth2 cultivated in rich medium supplemented with 3 g/L laminarin. (D) RT-qPCR detection of the expression of genes shown in panel C. Three replicates were performed for each condition. The locus tag and its corresponding encoding product were shown with the heat map. The heat map is generated by Heml 1.0.3.3. The numbers in panels A and C represent multiple differences in gene expression (by taking $\log_2$ values).

Figure 5. Genomic organization of bacteriophages released from *Lentisphaerae* strains WC36 and zth2 cultured in rich medium supplemented with polysaccharide. (A) Schematic of the genomic composition of Phage-WC36-1 and Phage-zth2-1. (B) A diagram showing the genomic composition of Phage-WC36-2. (C) The genomic composition of Phage-zth2-2. Arrows represent different ORFs and the direction of transcription. The main putative gene products of the phages are shown, and the numbers in brackets indicate the numbers of amino acids within each ORF. Hypothetical proteins are indicated with gray arrows, structural modules are indicated by green arrows, the replication module is indicated by blue-grey arrows, the regulatory module is indicated by golden arrows, the assembly and secretion modules are indicated by blue arrows and potential AMGs encoding proteins associated with polysaccharide transport and degradation are indicated by red arrows. The size of the phage genomes is shown behind each gene cluster.

Figure 5—figure supplement 1. Comparative genome analysis between the Phage-WC36-1 and Phage-zth2-1.

Figure 5—figure supplement 2. Phylogenetic analysis of Phage-WC36-1 and related phages. (A) Maximum likelihood phylogenetic tree of single-stranded DNA-binding protein sequences from phage-WC36-1 and some related phages. *Chlamydia pneumoniae* J138 was used as the outgroup. (B) Maximum likelihood phylogenetic tree of Zot protein sequences from phage-WC36-1 and some related *Tubulavirales* phages. *Escherichia coli* was used as the outgroup. Bootstrap values (%) > 50 (A) and >80 (B) are indicated at the base of each node with the gray dots (expressed as percentages of 1000 replications). The accession numbers of phages encoding single-stranded DNA-binding proteins and Zot proteins are given after the phage names.

Figure 5—figure supplement 3. Maximum likelihood phylogenetic tree of terL protein sequences from Phage-WC36-2, Phage-zth2-2, and some related *Caudoviricetes* phages. *Cytomegalovirus* phage AD169 was used as the outgroup. Bootstrap values (%) > 80 are indicated at the base of each node with the gray dots (expressed as percentages of 1000 replications). The accession numbers of phages encoding terL proteins are given after the names of the phages.

Supplementary file 1. Annotations of the transcriptome data of Lentisphaerae strain zth2 cultured in rich medium supplemented with or without 3 g/L laminarin. "Rich" indicates strain zth2 cultivated in rich medium; "Lam" indicates strain zth2 cultivated in rich medium supplemented with 3 g/L laminarin.

Supplementary file 2. Annotations of the Phage-WC36-1 and Phage-zth2-1 genome.

Supplementary file 3. Annotations of the Phage-WC36-2 genome.

Supplementary file 4. Annotations of the Phage-zth2-2 genome.

Supplementary file 5. Accession numbers of strain WC36, strain zth2, some *Planctomycetes-Verrucomicrobia-Chlamydia* (PVC) group bacteria, and *Bacillus cereus* ATCC 14579.

Supplementary file 6. Primers used for RT-qPCR.

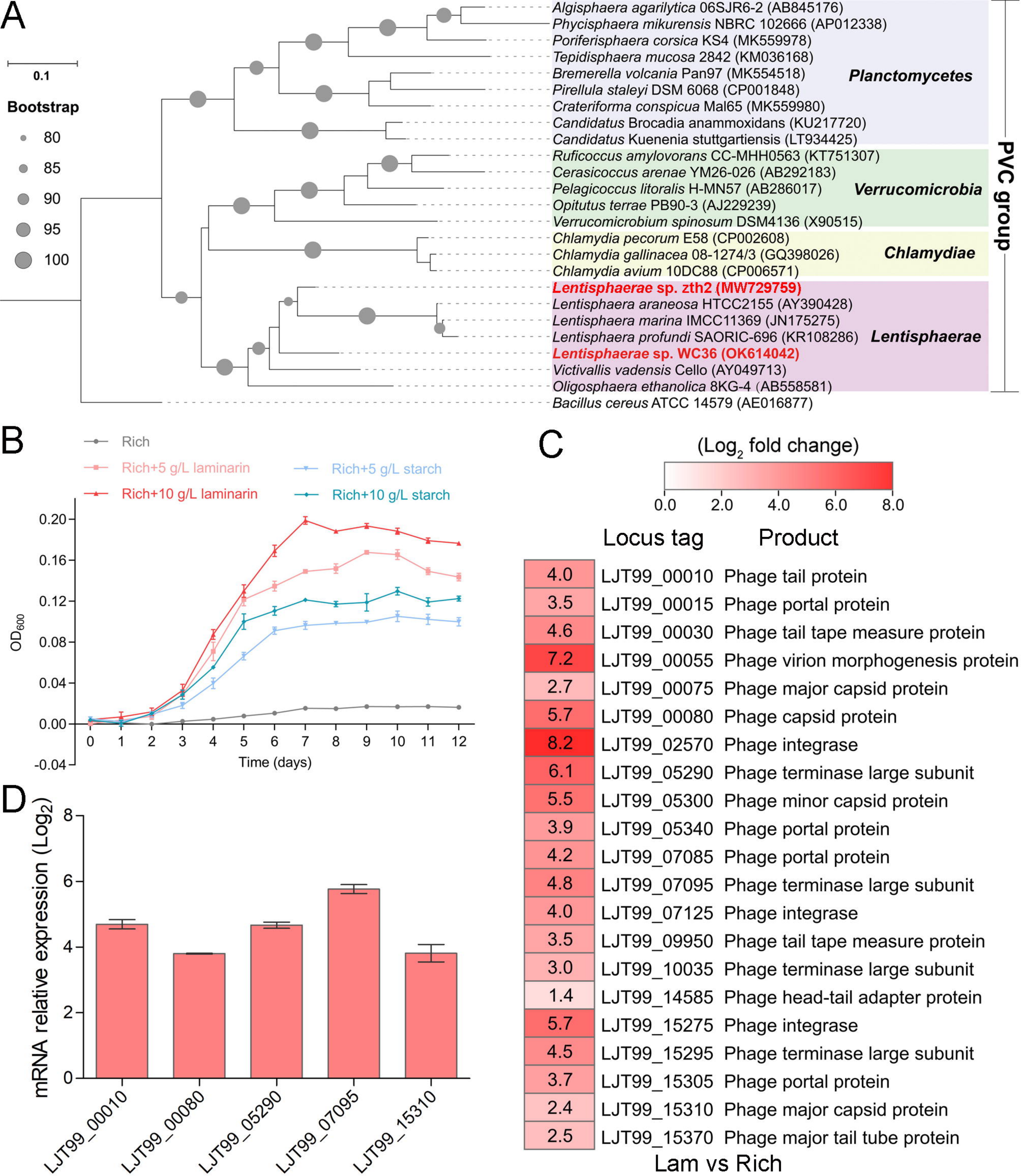
A
0.1
Bootstrap
80
85
90
95
100
Algisphaera agarilytica 06SJR6-2 (AB845176)
Phycisphaera mikurensis NBRC 102666 (AP012338)
Poriferisphaera corsica KS4 (MK559978)
Tepidisphaera mucosa 2842 (KM036168)
Bremerella volcania Pan97 (MK554518)
Pirellula staleyi DSM 6068 (CP001848)
Crateriforma conspicua Mal65 (MK559980)
Candidatus Brocadia anammoxidans (KU217720)
Candidatus Kuenenia stuttgartiensis (LT934425)
Planctomycetes
Ruficoccus amylovorans CC-MHH0563 (KT751307)
Cerasicoccus arenae YM26-026 (AB292183)
Pelagicoccus litoralis H-MN57 (AB286017)
Opitutus terrae PB90-3 (AJ229239)
Verrucomicrobium spinosum DSM4136 (X90515)
Verrucomicrobia
Chlamydia pecorum E58 (CP002608)
Chlamydia gallinacea 08-1274/3 (GQ398026)
Chlamydia avium 10DC88 (CP006571)
Chlamydiae
Lentisphaerae sp. zth2 (MW729759)
Lentisphaera araneosa HTCC2155 (AY390428)
Lentisphaera marina IMCC11369 (JN175275)
Lentisphaera profundi SAORIC-696 (KR108286)
Lentisphaerae sp. WC36 (OK614042)
Victivallis vadensis Cello (AY049713)
Oligosphaera ethanolica 8KG-4 (AB558581)
Lentisphaerae
Bacillus cereus ATCC 14579 (AE016877)
PVC group
B
Rich
Rich+5 g/L laminarin
Rich+10 g/L laminarin
Rich+5 g/L starch
Rich+10 g/L starch
OD600
Time (days)
C
(Log2 fold change)
0.0
2.0
4.0
6.0
8.0
Locus tag
Product
4.0 LJT99_00010 Phage tail protein
3.5 LJT99_00015 Phage portal protein
4.6 LJT99_00030 Phage tail tape measure protein
7.2 LJT99_00055 Phage virion morphogenesis protein
2.7 LJT99_00075 Phage major capsid protein
5.7 LJT99_00080 Phage capsid protein
8.2 LJT99_02570 Phage integrase
6.1 LJT99_05290 Phage terminase large subunit
5.5 LJT99_05300 Phage minor capsid protein
3.9 LJT99_05340 Phage portal protein
4.2 LJT99_07085 Phage portal protein
4.8 LJT99_07095 Phage terminase large subunit
4.0 LJT99_07125 Phage integrase
3.5 LJT99_09950 Phage tail tape measure protein
3.0 LJT99_10035 Phage terminase large subunit
1.4 LJT99_14585 Phage head-tail adapter protein
5.7 LJT99_15275 Phage integrase
4.5 LJT99_15295 Phage terminase large subunit
3.7 LJT99_15305 Phage portal protein
2.4 LJT99_15310 Phage major capsid protein
2.5 LJT99_15370 Phage major tail tube protein
Lam vs Rich
D
mRNA relative expression (Log2)
LJT99_00010
LJT99_00080
LJT99_05290
LJT99_07095
LJT99_15310

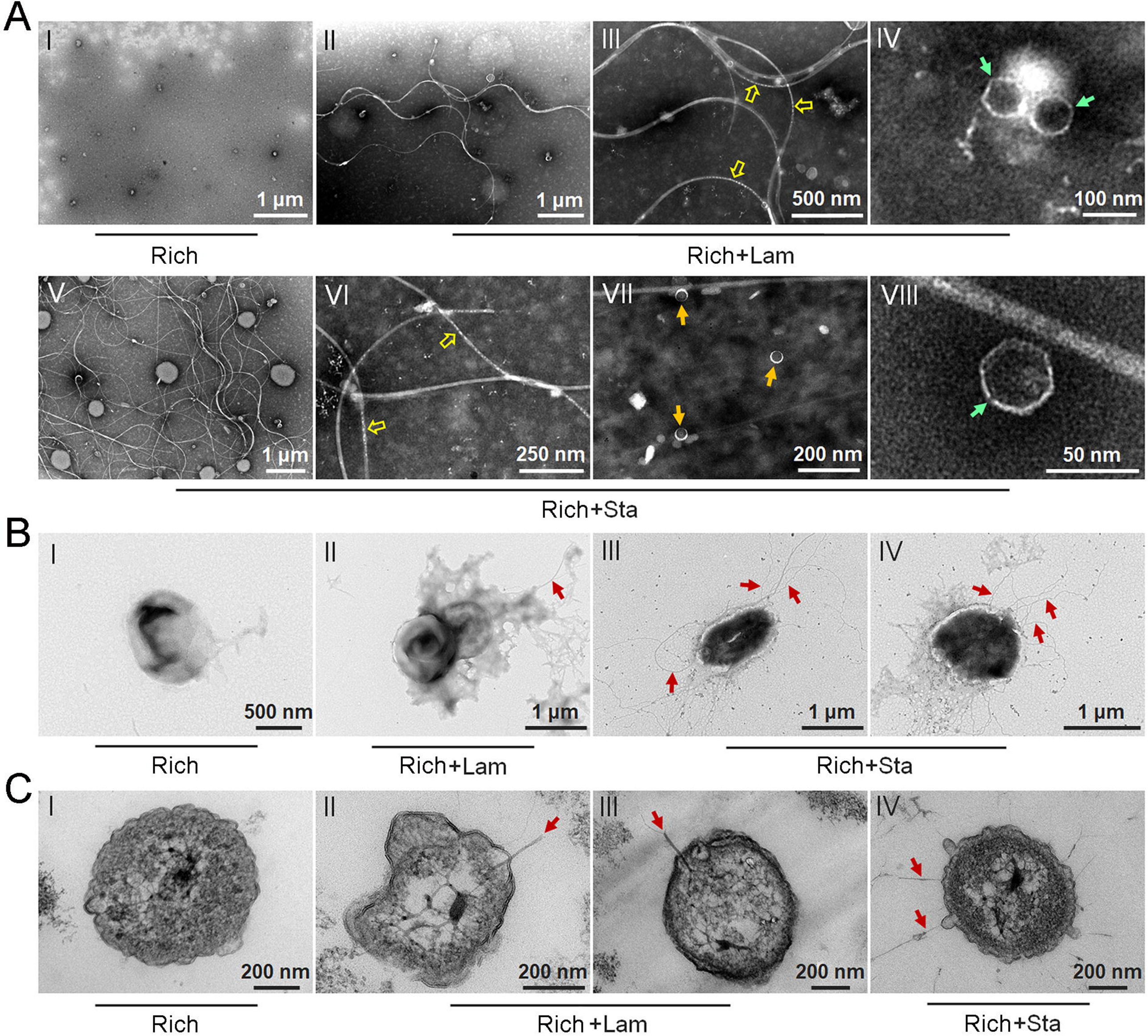
A
I
1 μm
II
1 μm
III
500 nm
IV
100 nm
Rich
Rich+Lam
V
1 μm
VI
250 nm
VII
200 nm
VIII
50 nm
Rich+Sta
B
I
500 nm
II
1 μm
III
1 μm
IV
1 μm
Rich
Rich+Lam
Rich+Sta
C
I
200 nm
II
200 nm
III
200 nm
IV
200 nm
Rich
Rich +Lam
Rich+Sta

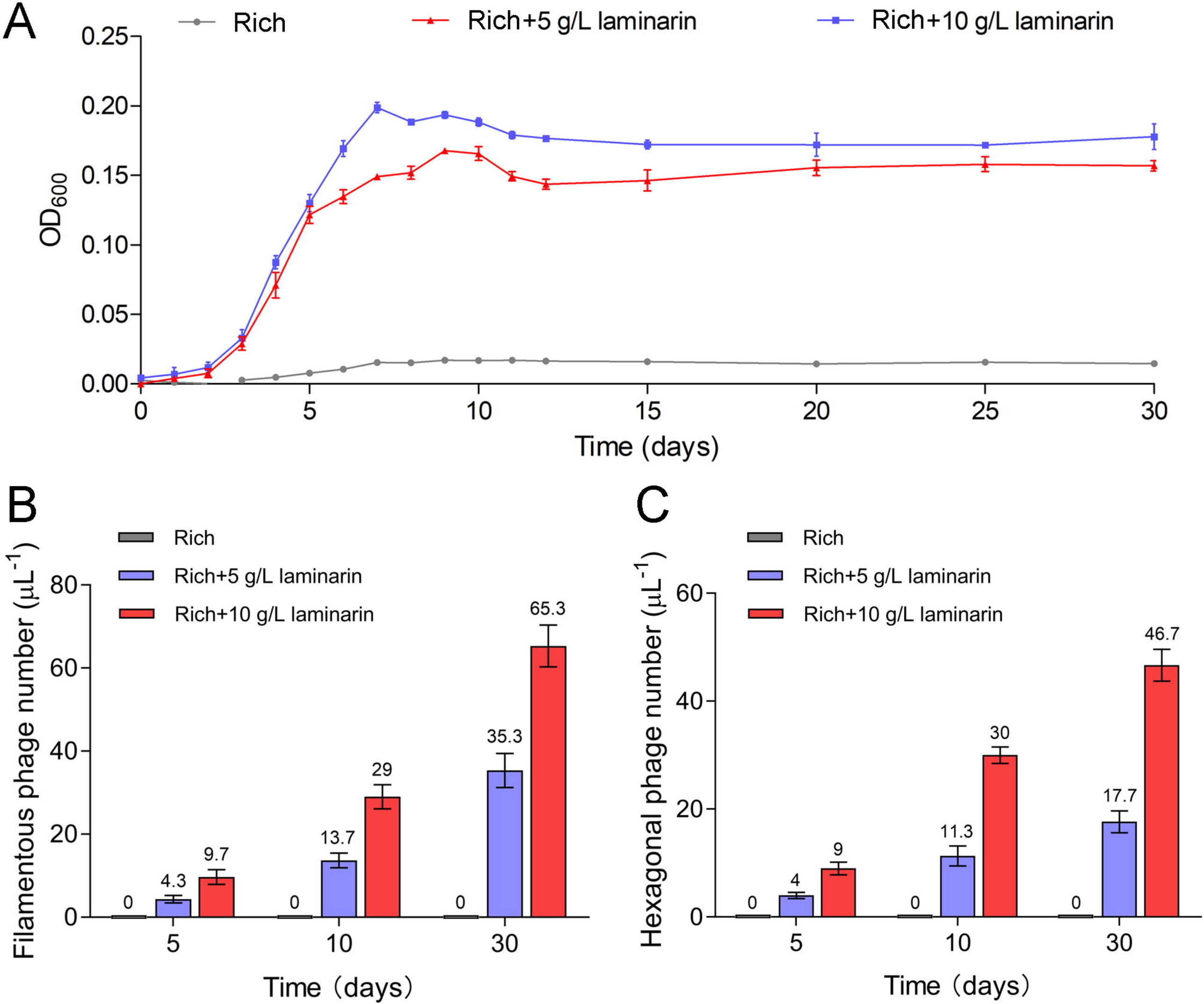
A
Rich
Rich+5 g/L laminarin
Rich+10 g/L laminarin
OD600
0.25
0.20
0.15
0.10
0.05
0.00
0
5
10
15
20
25
30
Time (days)
B
Rich
Rich+5 g/L laminarin
Rich+10 g/L laminarin
Filamentous phage number (μL-1)
80
60
40
20
0
0
4.3
9.7
0
13.7
29
0
35.3
65.3
5
10
30
Time（days）
C
Rich
Rich+5 g/L laminarin
Rich+10 g/L laminarin
Hexagonal phage number (μL-1)
60
40
20
0
0
4
9
0
11.3
30
0
17.7
46.7
5
10
30
Time（days）

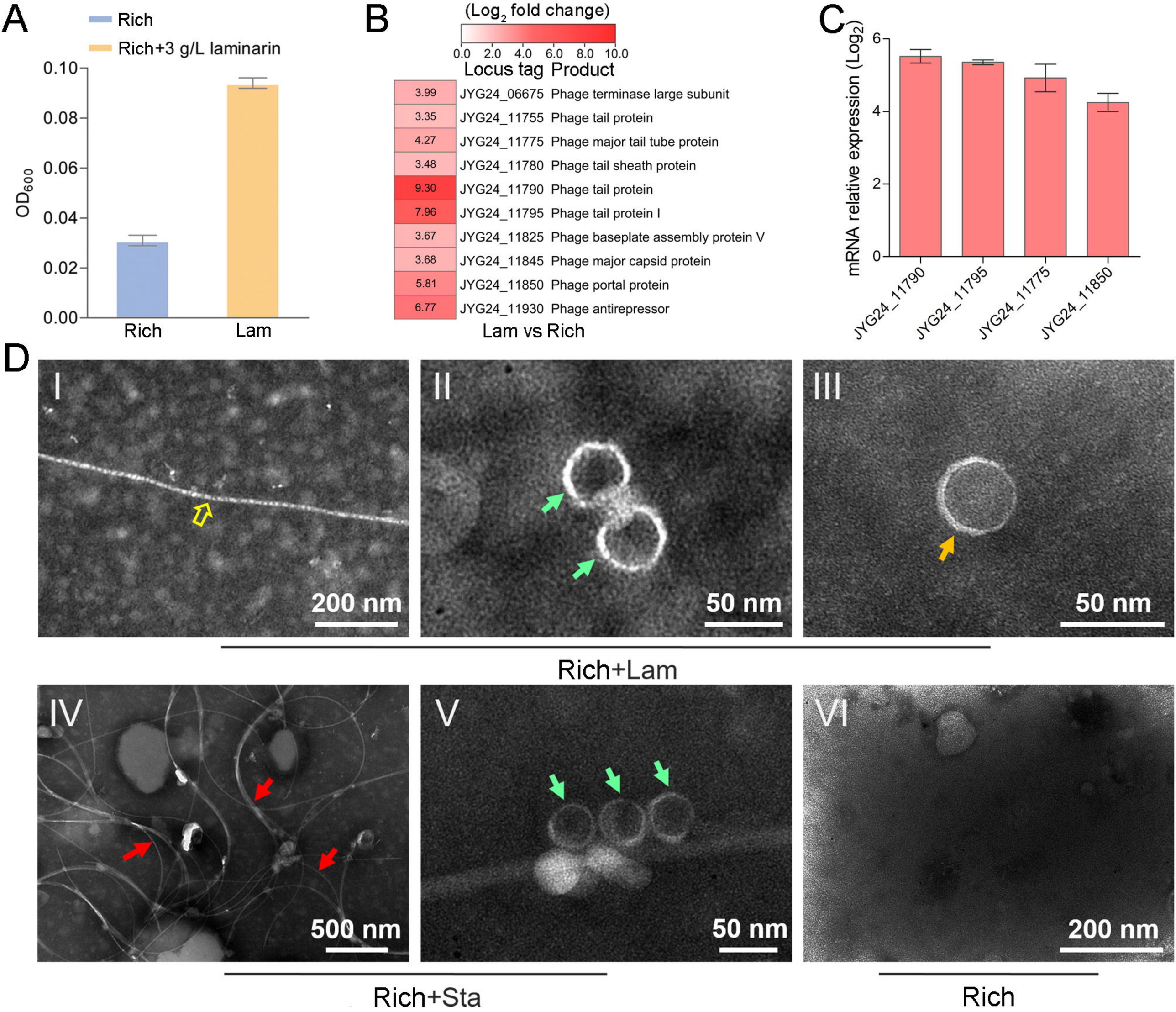
A
Rich
Rich+3 g/L laminarin
OD600
0.10
0.08
0.06
0.04
0.02
0.00
Rich
Lam
B
(Log2 fold change)
0.0 2.0 4.0 6.0 8.0 10.0
Locus tag Product
3.99 JYG24_06675 Phage terminase large subunit
3.35 JYG24_11755 Phage tail protein
4.27 JYG24_11775 Phage major tail tube protein
3.48 JYG24_11780 Phage tail sheath protein
9.30 JYG24_11790 Phage tail protein
7.96 JYG24_11795 Phage tail protein I
3.67 JYG24_11825 Phage baseplate assembly protein V
3.68 JYG24_11845 Phage major capsid protein
5.81 JYG24_11850 Phage portal protein
6.77 JYG24_11930 Phage antirepressor
Lam vs Rich
C
mRNA relative expression (Log2)
6
4
2
0
JYG24_11790
JYG24_11795
JYG24_11775
JYG24_11850
D
I
200 nm
II
50 nm
III
50 nm
Rich+Lam
IV
500 nm
V
50 nm
VI
200 nm
Rich+Sta
Rich

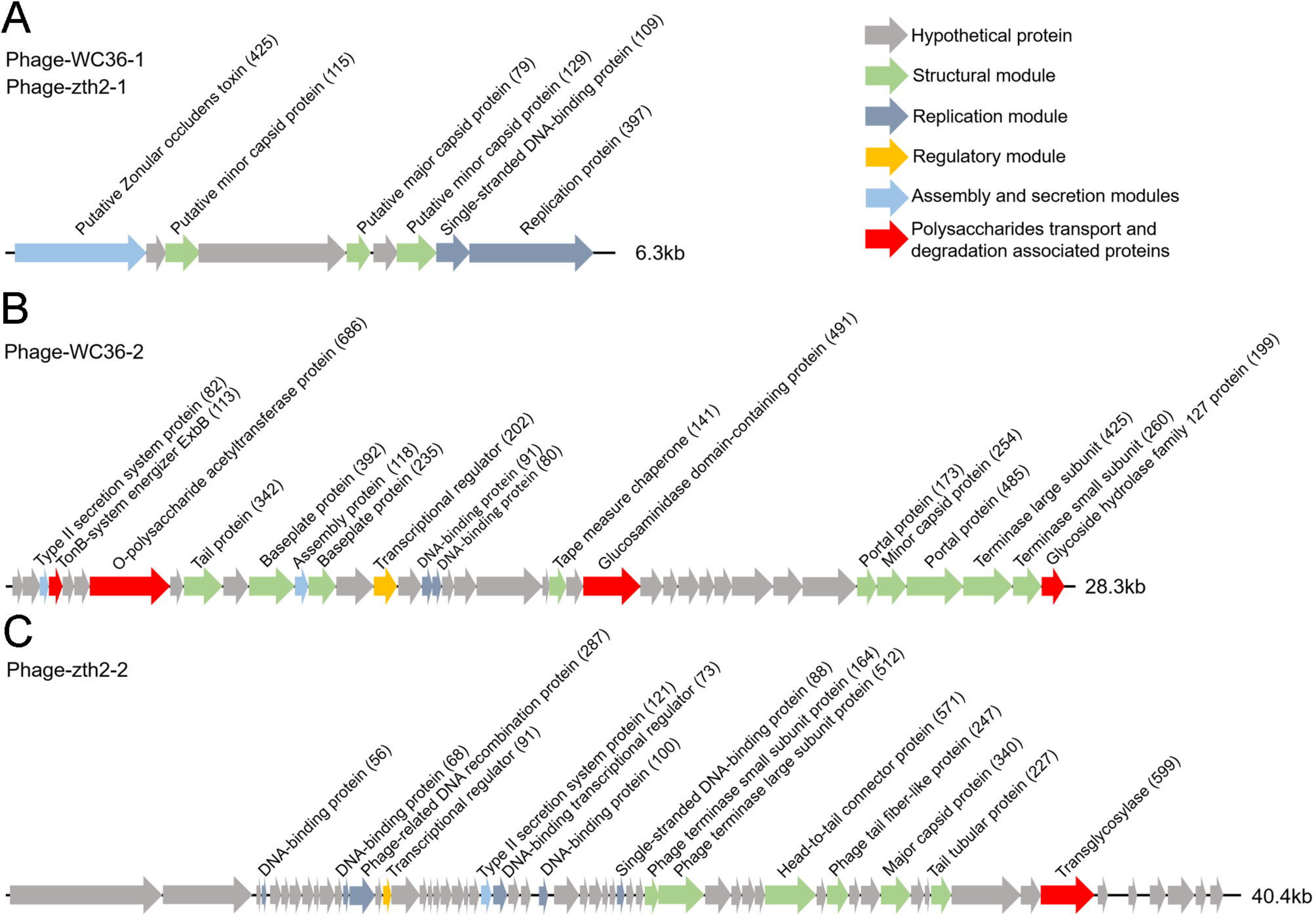
A
Phage-WC36-1
Phage-zth2-1
Putative Zonular occludens toxin (425)
Putative minor capsid protein (115)
Putative major capsid protein (79)
Putative minor capsid protein (129)
Single-stranded DNA-binding protein (109)
Replication protein (397)
6.3kb
Hypothetical protein
Structural module
Replication module
Regulatory module
Assembly and secretion modules
Polysaccharides transport and degradation associated proteins
B
Phage-WC36-2
Type II secretion system protein (82)
TonB-system energizer ExbB (113)
O-polysaccharide acetyltransferase protein (686)
Tail protein (342)
Baseplate protein (392)
Assembly protein (118)
Baseplate protein (235)
Transcriptional regulator (202)
DNA-binding protein (91)
DNA-binding protein (80)
Tape measure chaperone (141)
Glucosaminidase domain-containing protein (491)
Portal protein (173)
Minor capsid protein (254)
Portal protein (485)
Terminase large subunit (425)
Terminase small subunit (260)
Glycoside hydrolase family 127 protein (199)
28.3kb
C
Phage-zth2-2
DNA-binding protein (56)
DNA-binding protein (68)
Phage-related DNA recombination protein (287)
Transcriptional regulator (91)
Type II secretion system protein (121)
DNA-binding transcriptional regulator (73)
DNA-binding protein (100)
Single-stranded DNA-binding protein (88)
Phage terminase small subunit protein (164)
Phage terminase large subunit protein (512)
Head-to-tail connector protein (571)
Phage tail fiber-like protein (247)
Major capsid protein (340)
Tail tubular protein (227)
Transglycosylase (599)
40.4kb